Alloying effect of Nickel-Cobalt based binary metal catalysts supported on α-alumina for ammonia decomposition

Naohiro Shimoda*†, Ryo Yoshimura, Takahiro Nukui, Shigeo Satokawa*

Department of Materials and Life Science, Faculty of Science and Technology, Seikei University, 3-3-1 Kichijoji-kitamachi, Musashino-shi, Tokyo, 180-8633, Japan

Abstract

The development of a base metal catalyst which shows high performance for the ammonia (NH_3) decomposition have been conducted. For the Ni and Co based catalysts using α-Al_2O_3 as a support, the performance of the single metal catalysts was lower than that of the γ-Al_2O_3 supported catalysts. However, its performance was greatly improved by using a binary metal catalyst system. Based on the XRD analysis, it was found that Ni and Co supported on α-Al_2O_3 were alloyed. TEM observation confirmed that the metal particle size in the α-Al_2O_3 supported Ni-Co catalyst is smaller than that of the single metal catalysts (Ni/α-Al_2O_3 or Co/α-Al_2O_3). Furthermore, *in-situ* XRD and H_2-TPR measurements revealed that the Ni-Co alloy forms during the reduction process. The optimum mixing ratio of Ni and Co components was 1:1, and the optimum pre-reduction temperature before the performance test was 600 °C. Studies on the differences of support oxides proved that the improvement effect by alloying can be similarly obtained with the SiO_2 supported catalyst, indicating that the catalyst using the support with less interaction between the active metal and the support is more likely to obtain the performance improvement effect by alloying.

Keywords: Ammonia decomposition; Nickel; Cobalt; Alumina support, Alloying effect

Introduction

In recent years, hydrogen (H_2) fuel which does not emit carbon dioxide (CO_2) at combustion time is attracting attention from the viewpoint of environmental problems and energy problems. However, H_2 has the disadvantage of being difficult to store and transport (Becherif et al., 2015). Therefore, ammonia (NH_3) has recently attracted as one of the alternative energy carriers. Especially, NH_3 has many advantages such as liquefaction at normal temperature, high hydrogen content, and non-carbon-containing substances so that no CO_2 is generated at the time of decomposition. When decomposing NH_3 into H_2 (Eq. (1)), it is necessary to decompose on-site. Therefore, various catalysts that is active for the NH_3 decomposition reaction have been studied widely.

$$2NH_3 \rightarrow N_2 + 3H_2 \quad \Delta rH^\circ = 46\ kJ\ mol^{-1} \quad (1)$$

The history of NH_3 decomposition process is old, and Fe based catalyst was mainly employed (Ertl et al., 1980). After that, noble metals such as Ru and Rh, base metals such as Ni, Co, Fe and Mo, some carbides such as MoC and VC, some nitrides such as MoN_X and FeN_X (Hashimoto et al., 2000; Yin et al., 2004b; Choi, 1999; Liang et al., 2000) were studied as the active species of NH_3 decomposition catalyst. Among these catalysts, Ni and Ru based catalysts were found to exhibit high activity (Liu et al., 2007; Duan et al., 2013), Ru based catalyst have higher activity than Ni base catalyst (Choudhary et al., 2001). The metal oxide

Received on MM DD, YYYY; accepted on MM DD, YYYY

Correspondence concerning this article should be addressed to Naohiro Shimoda (E-mail: shimoda@tokushima-u.ac.jp) and Shigeo Satokawa (E-mail: satokawa@st.seikei.ac.jp)

†*Present address: Department of Applied Chemistry, Graduate School of Technology, Industrial and Social Sciences, Tokushima University, 2-1 Minamijosanjima, Tokushima-shi, Tokushima 770-8506, Japan*

used as a support of the catalyst is considered to be oxides of elements belonging to periodic tables 2 to 5 and 12 to 15. Indeed, many single metal oxides such as SiO_2, Al_2O_3 (Choudhary et al., 2001), ZrO_2 (Yin et al., 2006), MgO (Zhang et al., 2006), and Pr_6O_{11} (Nagaoka et al., 2010) are studied. As another support material, carbon based supports such as carbon nanotubes (CNTs) and graphite carbon black (GC) (Yin et al., 2004a; Li et al., 2007), and binary metal oxides such as Mg-Al hydrotalcite type compounds (Sato et al., 2017), $[Ca_{24}Al_{28}O_{64}]^{4+}(e^-)^4$ (Hayashi et al., 2013), and $CeZrO_2$ (Deng et al., 2012) have been also reported.

In the NH_3 decomposition reaction, NH_3 molecules adsorb and dissociate on the surface of the active metal, resulting in adsorbed N and H atoms. Subsequently, they associate with each other and desorb as N_2 and H_2 molecules (Hashimoto et al., 2000; Liang et al., 2000). According to the simulation study by a density functional theory (DFT) method, the reaction mechanism of NH_3 decomposition is proposed as follows: Over Ni and Co based catalysts, NH_3 molecules first adsorb to the top of one metal atom first, and then spillovers while increasing the number of metal atoms coordinated each time an H atom desorbs. In these studies, the rate-limiting step of NH_3 decomposition reaction is considered to be binding and desorption (recombination desorption) of adsorbed N atoms. Therefore, the supports that gives electrons to active metals are suitable, because the electron back donation leads to the enhancement of desorption of N atoms. Indeed, it is reported that the basic components can electron-donate to the active metals and lead to an improvement in the activity, and high performance catalysts to which an alkali metal such as K, Cs, and Ba is added have been reported (Raróg-Pilecka et al., 2003; Duan et al., 2012; Okura et al., 2015; Nagaoka et al., 2014). Additionally, there is a report that alkaline earth metals such as Ba are used as a structure promoter, and alkali metals such as K and Cs have a role as an electronic accelerator (Yin et al., 2006). In addition, it is reported that rare earth oxides are strongly basic and have been used as supports for NH_3 decomposition catalysts, and the activity can be further improved with a promoter such as K component (Nagaoka et al., 2014). Furthermore, carbon-based materials that are electron rich are considered to be excellent supports, and it is reported that Ru based catalysts supported on carbon nanotubes possess a high metal dispersion and are particularly active (Yin et al., 2004b; Huang et al., 2013).

Noble metal based catalysts using Ru and Rh can obtain an excellent performance in NH_3 decomposition reaction, but it is a problem that they are expensive. For this reason, in the present study, we have focused attention on base metal catalysts with active species of Ni, Co, and Fe, which are base metals but have relatively high performance. Furthermore, by using an alloying catalyst, the arrangement of the metal species is considered to be changed. As a result, it is expected that the bonding distance and electron arrangement between the adsorbed nitrogen atoms and the metal are changed, leading to easy cleavage of the bond between the nitrogen atom and the metal. Therefore, we have evaluated the performance of binary metal catalyst combining three metals of Ni, Co and Fe for NH_3 decomposition reaction.

1. Experimental

1.1. Catalyst preparation

All the catalysts used in this work were prepared by the impregnation method. As supports, γ-Al_2O_3 (BET surface area: 148 m^2 g^{-1}) was provided from Japan Reference Catalysis (JRC-ALO-8) and α-Al_2O_3 (BET surface area: 3 m^2 g^{-1}) was prepared from AlOOH (Sasol, CATAPAL 200) via the heat treatment in air at 1300 °C for 2 h. In addition, SiO_2 (Fuji-Silicia, CARiACT Q-50, BET surface are: 73 m^2 g^{-1}) and TiO_2 (Evonik Degussa, P25, BET surface are: 3 m^2 g^{-1}) were used as supports. An aqueous solution of nickel (II) nitrate hexahydrate ($Ni(NO_3)_2{\cdot}6H_2O$, Kanto Chemical Co.), cobalt (II) nitrate hexahydrate ($Co(NO_3)_2{\cdot}6H_2O$, Kanto Chemical Co.), and iron (III) nitrate hexahydrate ($Fe(NO_3)_3{\cdot}6H_2O$, Kanto Chemical Co.) were used as each metal source. The

metal content for all the prepared catalysts was adjusted to 10wt% in their metallic state. In the case of binary metal catalyst preparation, total weight ratio of both metals was 10 wt% in their metallic state. With respect to mixing ratio, the molar ratio of both metals appropriately changed. The obtained samples were calcined in air at 600 °C for 2 h and then pressed, crushed, and sieved to particle size of 150 to 250 μm for the catalytic performance tests of NH_3 decomposition.

1.2. Catalytic performance test of NH_3 decomposition

Catalytic performance tests of NH_3 decomposition were carried out in a fixed-bed flow reactor (*i.d.* 6 mm) at 400-600 °C under atmospheric pressure. The 50 mg of each catalyst was set in the reactor and then reduced in 10% H_2/N_2 (80 mL min^{-1}) at 600 °C for 5 h prior to the performance test. A reaction gas mixture of 1.02% NH_3/Ar was fed to the catalyst bed at the total flow rate of 120 mL min^{-1}. The contact time (W/F: weigh of catalyst / flow rate of reaction gas) was 2.45 kg-cat s L-NH_3^{-1} (0.0245 kg-cat s L-$total^{-1}$). The dry gaseous compositions of the inlet and outlet gases were analyzed using a JASCO FT-IR 4200, non-dispersive infrared spectroscopy (ND-IR) apparatus equipped with a 2 L gas cell.

1.3. Catalyst characterization

1.3.1. X-ray diffraction (XRD)

The crystalline phase of the catalysts was determined by powder X-ray diffraction (XRD, Ultima IV, Rigaku) equipped with a D/teX Ultra detector (Ni-filtered Cu Kα radiation, λ = 1.54 Å). The typical working conditions, such as the acceleration voltage and current were 40 kV and 40 mA. The lattice plane distance (d) of (111) plane metallic Ni and Co phases was determined by the Bragg's equation (Eq. (2)).

$$d = \frac{\lambda}{2\sin\theta} \qquad (2)$$

where λ is the X-ray wavelength (0.154 nm), and θ is the Bragg angle.

1.3.2. *In-situ* XRD

Variations in crystal structure of metal species during the high temperature reduction process were investigated by *in-situ* XRD measurement (Ultima IV, Rigaku) equipment with an atmosphere controllable cell. The XRD measurement was conducted at 50 °C, 400 °C, 500 °C, 600 °C, and 700 °C in *ca.* 4% H_2/Ar. The measurement conditions are the same as the XRD measurement at room temperature in the 1.3.1 section.

1.3.3. H_2-temperature programmed reduction (H_2-TPR)

The H_2-TPR measurement was conducted using a BEL-CAT-ADVANCE (MicrotracBEL). Prior to measurement, the catalyst sample was preheated in air at 300 °C for 0.5 h and cooled down to 50 °C in He atmosphere. Subsequently, the sample was heated up to 900 °C in 4% H_2/Ar of 30 mL min^{-1} at a heating rate of 10 °C min^{-1}.

1.3.4. Transmission electron microscope (TEM)

The morphology of each catalyst was observed using a transmission electron microscope (TEM, JEM-2100F, JEOL). The operating voltage, emission current, and dark current were 200 kV, 230 μA, and 93–97 μA, respectively. The catalyst sample was crushed into powder and dispersed in ethanol with ultrasonic agitation, followed by transfer onto a copper grid.

1.3.5. Nitrous oxide pulse

To investigate the metal active sites in the catalyst, N_2O pulse measurement was carried out using a BEL-CAT-ADVANCE (MicrotracBEL) equipped with thermal conductivity detector. For pretreatment, the catalyst sample was initially reduced under 4% H_2/Ar atmosphere at 600 °C for

2 h prior to the measurement, and then cooled down to 50 °C in H_2 atmosphere. Subsequently, the 0.032 mL of N_2O was pulsed repeatedly to the sample until the amount of N_2O at the outlet reached a constant value at 50 °C in He atmosphere. The reduced metal species is oxidized by N_2O to produce N_2. The N_2 and N_2O in the outlet gas were separated using an active carbon column and the consumption amount of N_2O was determined.

2. Results and discussion

2.1. Catalytic performance of single metal catalysts

First, we have evaluated the performance of single metal catalysts using γ-Al_2O_3 as a support with the metal loading amount of 10 wt%. The NH_3 conversion for Ni/γ-Al_2O_3, Fe/γ-Al_2O_3, and Co/γ-Al_2O_3 catalysts are shown in Fig. 1A. The conversion reached ca. 100%, which is the equilibrium conversion, for Ni/γ-Al_2O_3 at ca. 550 °C and for Co/γ-Al_2O_3 at *ca.* 600 °C, respectively. But their conversions at the low temperature region were almost equivalent. In contrast, the Fe/γ-Al_2O_3 exhibited lower performance than the other catalysts. As a reference, the catalytic performance of 1.0 wt% Ru/γ-Al_2O_3 have been evaluated, resulting that the conversion reached equilibrium conversion at 450 °C (a result is not shown). Next, the performance tests have been also carried out for single metal catalysts using α-Al_2O_3 as a support in the same manner. The NH_3 conversion for Ni/α-Al_2O_3, Fe/α-Al_2O_3, and Co/α-Al_2O_3 catalysts are shown in Fig. 1B. There was no difference in the catalytic performance among three catalysts. From these results, it was found that the NH_3 decomposition performance at 500 °C is highest for Ni/γ-Al_2O_3 catalyst. Furthermore, in order to improve the NH_3 decomposition performance of these base metal-based catalysts, we have examined the use of binary metal catalysts in which the base metal catalysts are combined with each other.

2.2. Catalytic performance of binary metal catalysts

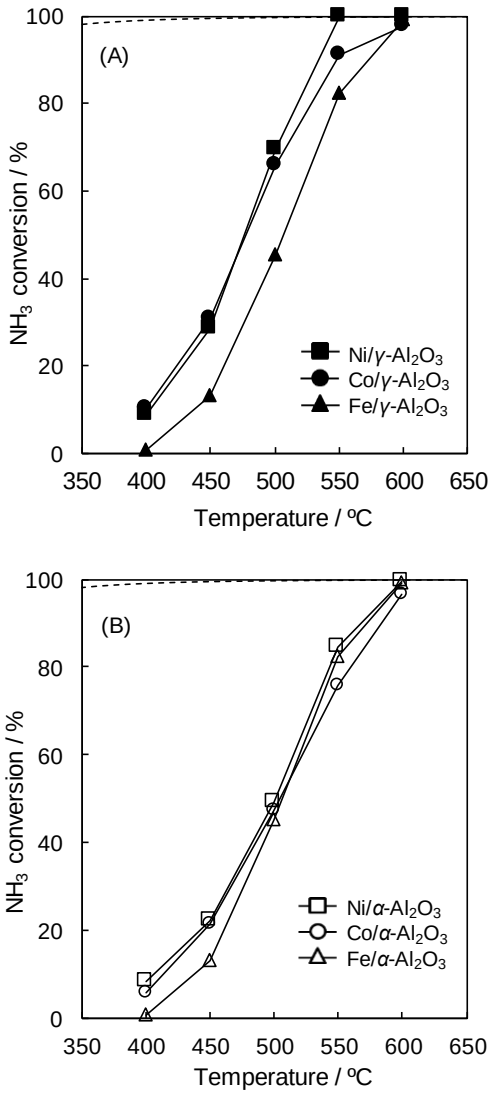

Fig. 1 NH_3 conversion for NH_3 decomposition over (A) γ-Al_2O_3 and (B) α-Al_2O_3 supported mono-metal catalysts: (square) Ni, (circle) Co, (triangle) Fe. Reaction conditions: 1.02% NH_3/Ar balance; W/F: 2.45 kg-cat s L-NH_3^{-1}; catalyst weight: 0.050 g. (dot-line) equilibrium NH_3 conversion.

The NH_3 conversion for the three catalysts such as Ni-Co/γ-Al_2O_3, Co-Fe/γ-Al_2O_3, and Ni-Fe/γ-Al_2O_3 are shown in Fig 2A. The total loading amount of metals was adjusted to 10wt% in their metallic state, and the molar ratio of metals was adjusted to 1:1. Among the γ-alumina supported catalysts, the performance of the Ni-Co/γ-Al_2O_3 and Ni-Fe/γ-Al_2O_3 were high and the performance

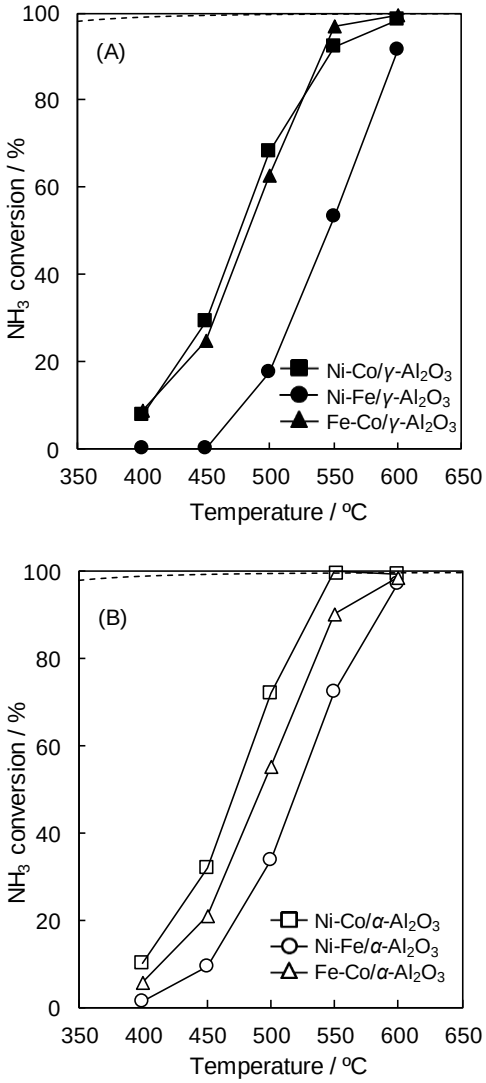

Fig. 2 NH_3 conversion for NH_3 decomposition over (A) γ-Al_2O_3 and (B) α-Al_2O_3 supported bi-metal catalysts: (square) Ni-Co, (circle) Ni-Fe, (triangle) Fe-Co. The molar ratio of both metals = 1:1. Reaction conditions: 1.02% NH_3/Ar balance; W/F: 2.45 kg-cat s L-NH_3^{-1}; catalyst weight: 0.050 g. (dot-line) equilibrium NH_3 conversion.

of the Fe-Co/γ-Al_2O_3 was significantly low. Similarly, the NH_3 conversion of binary metal catalysts such as Ni-Co/α-Al_2O_3, Co- Fe/α-Al_2O_3, and Ni-Fe/α-Al_2O_3 are shown in Fig. 2B. When α-Al_2O_3 was used as a support, we found that the performance of the binary metal catalyst of Ni and Co was the highest.

Considering the above results, particular attention was given to Ni catalysts and Co catalysts which exhibited high NH_3 decomposition performance. Fig. 3 represents the results of comparing the conversion of NH_3 at 500 °C for Ni and Co based catalysts. For the case of the γ-Al_2O_3 supported catalysts, the NH_3 conversions for the Ni/γ-Al_2O_3, Co/γ-Al_2O_3, and Ni-Co/γ-Al_2O_3 which are single metal catalysts are approximately 69%, 66%, and 68%, respectively, which were almost identical. In contrast, for the α-Al_2O_3 supported catalysts, the conversion of Ni/α-Al_2O_3 and Co/α-Al_2O_3 were as low as 50%, while the binary metal catalyst, Ni-Co/α-Al_2O_3, was *ca.* 73%, which was the highest conversion. Generally, in the reaction process over heterogeneous catalysts, the catalytic performance is considered to be high performance, as the metal dispersion of the active metal species is high, that is, the smaller the particle size. However, in this work, by using the Ni-Co binary metal catalyst, the catalyst with the α-Al_2O_3 support having a low specific surface area, which is generally expected to have low metal dispersion, showed the highest performance for NH_3 decomposition.

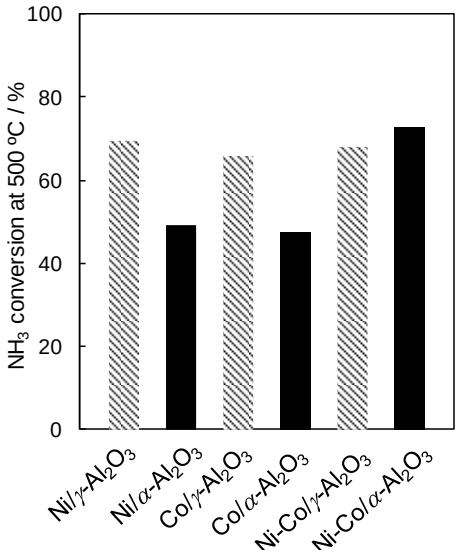

Fig. 3 NH_3 conversion at 500 ºC for Ni and Co based catalysts for NH_3 decomposition tests shown in Figs. 1 and 2.

2.3. Characterization of the catalyst

2.3.1. XRD

The XRD patterns of Ni/γ-Al_2O_3, Co/γ-Al_2O_3, and Ni-Co/γ-Al_2O_3 catalysts after the NH_3 decomposition tests are shown in Fig. 4A. It is noted that the diffraction peaks assigned to the γ-Al_2O_3 support in all catalysts were broad. No diffraction peak derived from the oxide phase of the active metal component was confirmed for all the catalysts, and the diffraction peaks derived from each metal component appeared. This indicates that the metal species as the active species was reduced from the oxide to the metal at 600 °C. It is expected that the diffraction peaks ascribed to Ni and Co metallic phases that are active metals will appear with considerably weak intensity at 2θ = *ca.* 44° and 51° for each catalyst. Indeed, for the Co containing catalysts (Ni-Co/γ-Al_2O_3 and Co/γ-Al_2O_3), the diffraction peaks assigned to Co metal or Co-Ni alloy appeared at *ca.* 44° and 51°. By contrast, the diffraction peaks assigned to Ni metal hardly appeared for the Ni/γ-Al_2O_3. We consider that the metal Ni species are considerably dispersed. In addition, since the peak intensities of Ni, Co, and Ni-Co phases for the XRD patterns of Ni-Co/γ-Al_2O_3 catalyst were weak, it is unclear that whether Ni-Co alloy phase was formed or not.

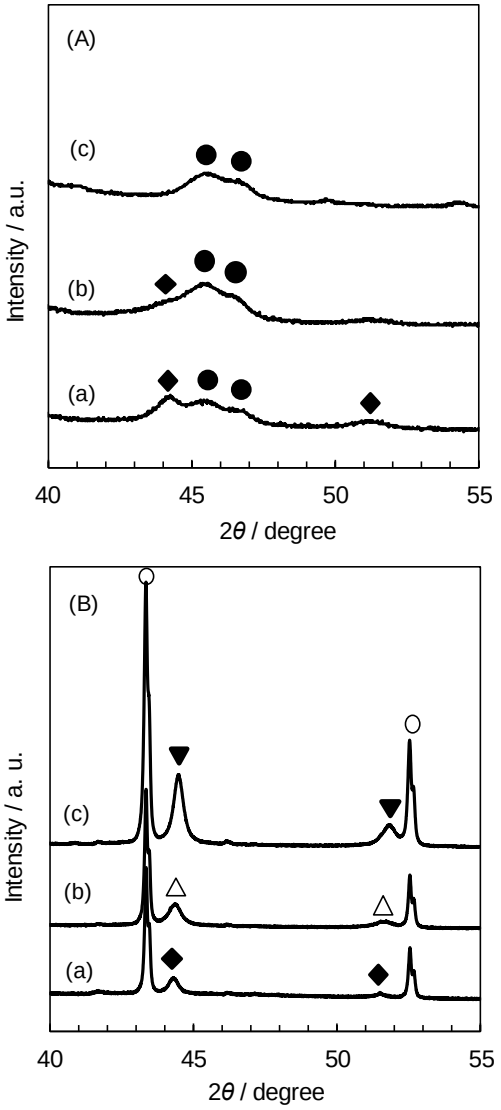

Fig. 4 XRD patterns of the spent Ni and Co based catalysts after NH_3 decomposition tests shown in Figs. 1 and 2: (A-a) Co/γ-Al_2O_3, (A-b) Ni-Co/γ-Al_2O_3, (A-c) Ni/γ-Al_2O_3, and (B-a) Co/α-Al_2O_3, (B-b) Ni-Co/α-Al_2O_3, (B-c) Ni/α-Al_2O_3. Symbols:(●) γ-Al_2O_3, (○) α-Al_2O_3, (◆) Co, (▼) Ni, (△) Ni-Co alloy.

Fig. 4B shows the XRD patterns of Ni/α-Al_2O_3, Co/α-Al_2O_3, and Ni-Co/α-Al_2O_3 catalysts after the NH_3 decomposition tests. For all the spent catalysts, the diffraction peaks attributed to each metal component as well as α-Al_2O_3 as a support were confirmed. The diffraction peaks derived from metallic Ni and Co phases appeared at *ca.* 45° and 51° for the Ni/α-Al_2O_3 and Co/α-Al_2O_3 catalysts. In addition, as compared with the results of the γ-Al_2O_3 supported catalysts, the difference in position of the diffraction peaks was clear for the α-Al_2O_3 supported catalysts. For the Ni-Co/α-Al_2O_3 catalyst, the diffraction peaks derived from metal components appeared at between the peak positions of metallic Ni and metallic Co phases. This result implied that the binary metal catalyst Ni-Co/α-Al_2O_3 is alloyed by the reduction treatment at 600 °C prior to the performance test.

2.3.2. H_2-TPR

Reduction behavior of single metal catalysts such as Ni/α-Al_2O_3, Co/α-Al_2O_3, and Fe/α-Al_2O_3 catalysts and a binary metal catalyst Ni-Co/α-Al_2O_3 catalyst after the preparation has been

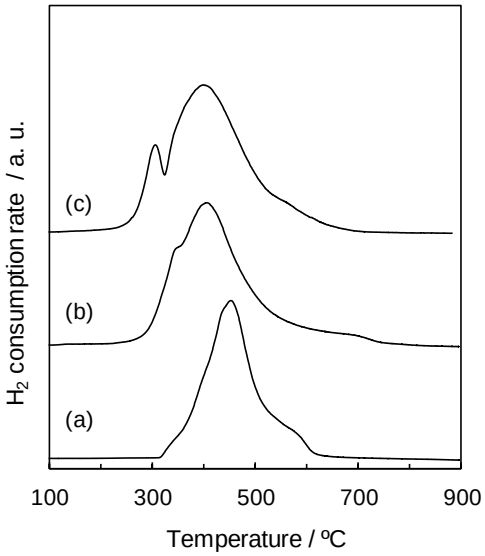

Fig. 5 H_2-TPR profiles of the prepared Ni and Co based catalysts: (a) Ni/α-Al_2O_3, (b) Co/α-Al_2O_3, (c) Ni-Co/α-Al_2O_3.

studied. We note that before TPR measurement, the metal component in the catalyst exists in oxidized state. Fig. 5a shows the H_2-TPR profile of the Ni/α-Al_2O_3 catalyst. The reduction peak attributed to the reduction of Ni species was observed at *ca.* 460 °C. In addition, small reduction peak was also confirmed at *ca.* 580 °C. As shown in Fig. 5b, for the Co/α-Al_2O_3 catalyst, two distinct reduction peaks attributed to the reduction of Co species were observed at *ca.* 340 °C and 410 °C, and the small peak was slightly observed at *ca.* 700 °C. These plurality of reduction peaks mean the presence of multiple reduction steps. For the reduction of Ni species in the supported catalysts, a peak separation is observed due to changes in the compound, the particle size, and the interaction with the support (Shimoda et al., 2018). For the reduction of Co species, there is a report of two reduction step in which Co_3O_4 is reduced to CoO and then reduced to metallic Co (Luisetto et al., 2012; Muñoz et al., 2014). In addition, there is a report that the reduction peak shifts to higher temperature by the interaction with alumina as a support (Shimoda et al., 2018). Fig. 5c shows the H_2-TPR profile of Ni-Co/α-Al_2O_3 catalyst. The reduction peaks appeared at *ca.* 310 °C, 410 °C, and 570 °C. It is reported that the reduction peak in the H_2-TPR profile occurs at a slightly lower

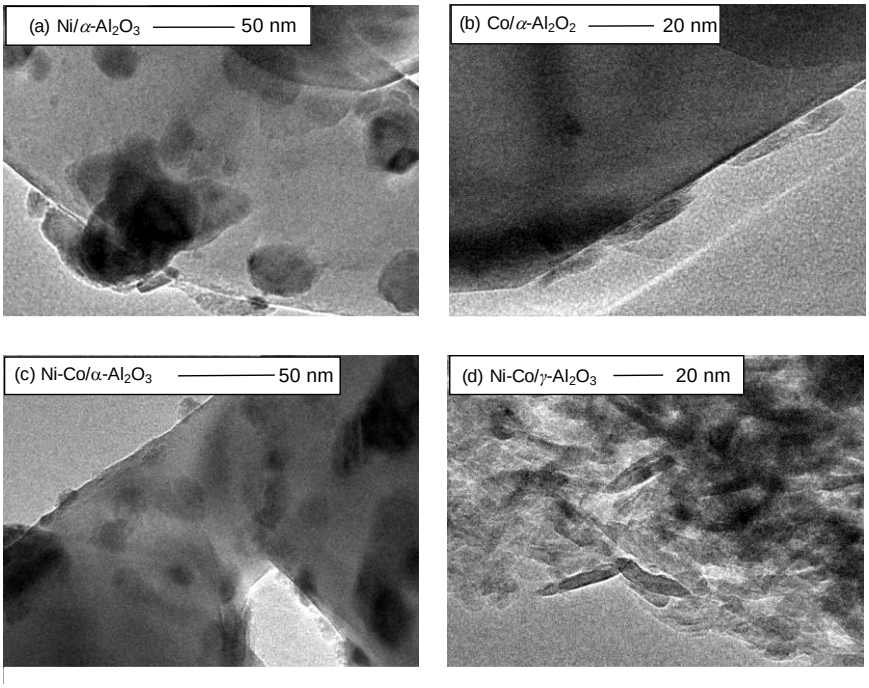

Fig. 6 TEM images of the spent catalysts: (a) Ni/α-Al_2O_3, (b) Co/α-Al_2O_3, (c) Ni-Co/α-Al_2O_3 , (d) Ni-Co/γ-Al_2O_3.

temperature in the formation process of Ni-Co alloy (Sengupta et al., 2014; Gonzalez-Delacruz et al., 2012), and the similar tendency was obtained in this reduction profile.

2.3.3. TEM observation

In order to confirm the particle size of the metal and the alloy state, the microstructure of the spent catalysts after the performance test was observed by TEM. It is noted that α-Al_2O_3 was large crystal grains with the size of several micrometers. From the TEM image of Ni/α-Al_2O_3 shown in Fig. 6a, it is found that the metal Ni particles in the Ni/α-Al_2O_3 catalyst are spherical and the size of the Ni particles was considerably scattered. From the TEM image of Co/α-Al_2O_3 shown in Fig. 6b, many Co particles were in a rod shape, and the average particle size was *ca.* 35 nm in length and *ca.* 15 nm in width. Fig. 6c represents the TEM image of Ni-Co/α-Al_2O_3. The size of the metal particles on the support was smaller and more uniform in size than those in the Ni/α-Al_2O_3. The average particle size was *ca.* 30 nm, but it was not possible to distinguish whether Ni and Co components were alloyed or not based on the TEM observation. By contrast, for the Ni-Co/γ-Al_2O_3 catalyst shown in Fig. 6d, the morphology of the alumina support varied significantly. The γ-Al_2O_3 has been reported to be acicular crystals, which is confirmed by the TEM observation in this work. The metal particles in the Ni-Co/γ-Al_2O_3 catalyst were quite small and it was difficult to distinguish shape and size.

2.3.4. N_2O pulse

Table 1 summarizes the amount of N_2O consumption for various α-Al_2O_3 supported catalysts in the N_2O pulse measurement. Consumption of a certain amount of N_2O was confirmed for all the catalysts. From these values, we tried to calculate the metal dispersion and the particle size of metallic Ni and Co, but they were largely different from the particle size by the TEM observation. For this reason, the number of active sites in the catalyst has been relatively compared

Table 1 Amount of N_2O consumption for the spent Ni and Co based catalysts after NH_3 decomposition shown in Figs. 1 and 2 and the TOF (turnover frequency) values for NH_3 decomposition at 500 °C.

N_2O consumption amount ($cm^3\ g^{-1}$)			
Support	Loading metal		
	Ni	Co	Ni-Co
α-Al_2O_3	0.40	0.23	0.78
γ-Al_2O_3	0.47	0.32	0.43
TOF (s^{-1})			
Support	Loading metal		
	Ni	Co	Ni-Co
α-Al_2O_3	0.50	0.83	0.37
γ-Al_2O_3	0.59	0.82	0.63

using N_2O consumption per 1 g of the catalyst. As a result, the consumption amount of N_2O for the Ni-Co/α-Al_2O_3 catalyst was 0.78 $cm^3\ g^{-1}$, which was larger than that of Ni/α-Al_2O_3 (0.40 $cm^3\ g^{-1}$) and of Co/α-Al_2O_3 (0.23 $cm^3\ g^{-1}$). These results suggest that the active metal is alloyed by the reduction treatment for a binary metal catalyst, and the particle size of its alloy becomes small. This is consistent with the fact that the metal particle size of the alloyed catalyst becomes smaller than that of the single metal catalysts in the TEM observation. In contrast, the amount of N_2O consumption for the γ-Al_2O_3 supported catalysts were 0.43 $cm^3\ g^{-1}$ for Ni-Co/γ-Al_2O_3, 0.47 $cm^3\ g^{-1}$ for Ni/γ-Al_2O_3, and 0.32 $cm^3\ g^{-1}$ for Co/γ-Al_2O_3, respectively. Comparing with the α-Al_2O_3 supported catalysts, the different in N_2O consumption amount between the γ-Al_2O_3 supported catalysts were small. This result indicates that the alloying effect by the reduction treatment at 600 °C prior to the performance test is small for the binary metal catalyst of Ni-Co/γ-Al_2O_3. Furthermore, when the TOF (turnover frequency) values at 500 °C for the α-Al_2O_3 supported catalysts were compared from

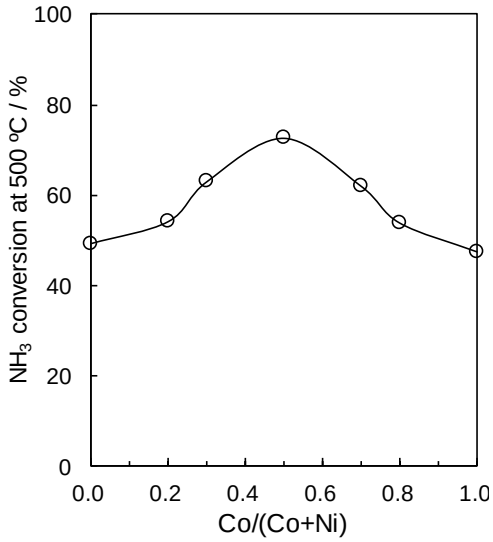

Fig. 7 Effect of molar ratio of Co/(Co+Ni) on NH_3 conversion at 500 ºC over Ni-Co/α-Al_2O_3 catalysts.

the obtained data, it was found that the order was Ni-Co/α-Al_2O_3 < Ni/α-Al_2O_3 < Co/α-Al_2O_3. This result implies that the effect of increasing the number of active sites mainly contributes to the improvement factor of the catalyst performance due to the binary metal catalyst than the electronic effect on the active sites.

2.4. NH_3 decomposition over Ni-Co based catalysts

2.4.1. Molar ration of Ni to Co

We have studied the composition ratio of Ni and Co to aim for further improvement of the binary metal catalysts of Ni and Co with the α-Al_2O_3 support which exhibited the highest performance. Various catalysts were prepared with the Co/(Co+Ni) of 0.0, 0.3, 0.5, 0.7, and 1.0 in terms of molar ratio of metal, and the NH_3 decomposition performance was compared (Fig. S1). In addition, Fig. 7 shows the comparison of the NH_3 conversion at 500 °C between various Ni-Co/α-Al_2O_3 catalysts. As a result, it was found that NH_3 conversion was the highest in the case of Co/(Co+Ni) = 0.5, and the binary metal catalysts showed better performance than the single metal catalysts. According to this result, we conclude the catalytic performance can be improved by complexing the two metals of Ni and Co components, that is, by the alloying effect.

2.4.2. Reduction treatment

In order to reveal the optimal temperature of the reduction treatment for the catalyst prior to the performance test, the Ni-Co/α-Al_2O_3 catalyst with the Co/(Co+Ni) of 0.5 was reduced at 500 °C, 600 °C, 700 °C, and 800 °C, and subsequently the NH_3 decomposition performance was evaluated (Fig. S2). The NH_3 conversion at 500 °C was 60% for the case with the reduction temperature of 800 °C, 65% for the case at 700 °C, 72% for the case at 600 °C, and 73% for the case at 500 °C, respectively. The NH_3 decomposition performance when the catalyst was reduced at 500 °C and 600 °C were almost identical and highest, indicating that the catalytic performance tends to decrease as the reduction temperature increases.

2.4.3. Crystalline phase of the catalyst

The XRD patterns of the Ni-Co/α-Al_2O_3 catalysts with the Co/(Co+Ni) of 0 to 1.0 after the performance test are shown in Fig. 8A. The diffraction peak ascribed to Co (111) plane appeared at *ca.* 44.3 ° for the Co/α-Al_2O_3, and the peak ascribed to Ni (111) plane appeared at *ca.* 44.5 ° for the Ni/α-Al_2O_3. The diffraction peak position for the Ni-Co/α-Al_2O_3 catalysts with different Ni to Co composition ratios were between those for the Co/α-Al_2O_3 and Ni/α-Al_2O_3 catalysts. The diffraction peak for the Ni-Co/α-Al_2O_3 catalysts shifted to the higher angle side as the amount of Ni content increased. In addition, all the diffraction peaks assigned to metal species appeared in the single-phase diffraction patterns. Therefore, it is considered that they exist in the solid solution state. The relationship between the composition ratio of Ni and Co and the lattice plane distance (d) based on each XRD peak is plotted as shown in Fig. 8B. It was found that the d value increases almost linearly as the amount of Co increases, which this trend applies to Vegard's law. In other words, it is implied that Ni and Co species in the binary metal catalysts after the NH_3

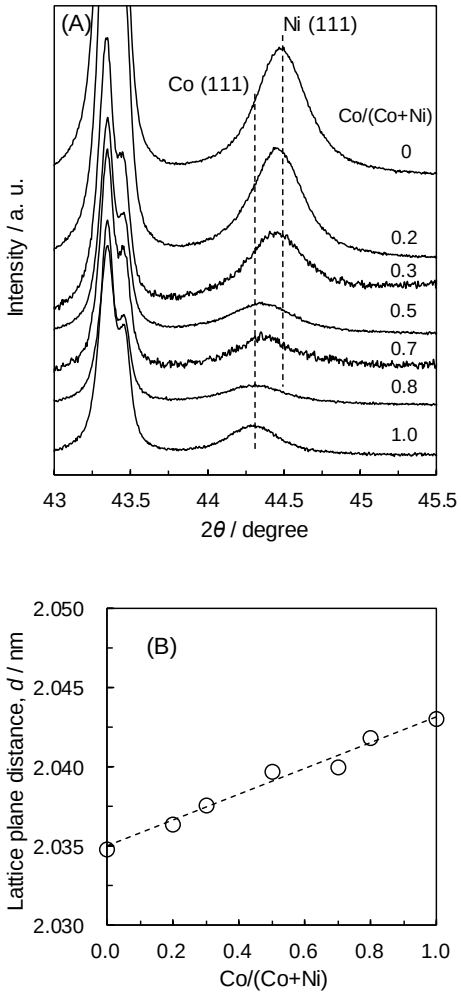

Fig. 8 (A) XRD patterns and (B) relationship between Co/(Co+Ni) and lattice plane distance for the spent Ni-Co/α-Al_2O_3 catalysts after NH_3 decomposition tests.

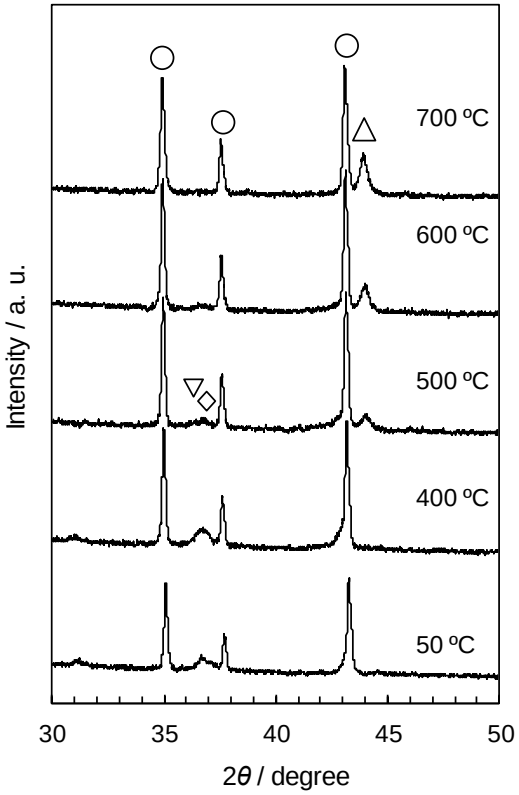

Fig. 9 *In-situ* high temperature XRD patterns for the prepared Ni-Co/α-Al_2O_3 catalyst with the Co/(Co+Ni) of 0.5. Symbols: (○) α-Al_2O_3, (◇) Co_3O_4, (▽) NiO, (△) Ni or Co. Measurement atmosphere: 4% H_2/Ar.

decomposition tests with the reduction treatment at 600 °C were solid-solved and alloyed.

The result of *in-situ* XRD measurement under the reduction atmosphere in 4% H_2/Ar at various temperatures for the Ni-Co/α-Al_2O_3 catalyst is shown in Fig. 9. At 50 ºC, in addition to the diffraction peak derived from the support, two peaks assigned to NiO phase and Co_3O_4 phase were observed 2θ = *ca.* 45 º separately. Since their peaks were independent from each other, two oxides are considered to be not solid solution in the oxide state. When the temperature was raised, the peaks of the oxides decreased and almost disappeared at 500 ºC, and the diffraction peak attributed to an alloy of Ni and Co appeared. Furthermore, when the temperature was increased to 600 ºC and 700 ºC, the peak intensity of the Ni-Co alloy increased and became sharp significantly. We conclude that Ni and Co species are considered to form a Ni-Co alloy during the reduction atmosphere at 600 ºC. It was reported that a Cu-Ni alloy was formed in the reduction process in Cu-Ni/SiO_2 in the previous study by Saw *et al.* (Saw et al., 2014), and the same phenomena may occur in the Ni-Co/α-Al_2O_3 system in our present study.

2.5. Arrhenius plot

For the NH_3 decomposition test using each catalyst, Arrhenius plots were prepared. From the data on the NH_3 conversion, it was assumed that the reaction was a primary reaction against NH_3,

and the reaction rate constant (k) and the apparent activation energy (Ea) were calculated. First, when the reaction rate formula is as follows:

$$r = -\frac{d}{dt}C = kC \quad (3)$$

where r is the reaction rate, C is the NH_3 concentration, and t is the reaction time. Here, Eq. (3) can be transformed into Eq. (4).

$$-\ln\frac{C0}{C} = kt \quad (4)$$

where C_0 is initial NH_3 concentration. Since (C_0-C)/C_0 means the conversion, letting the NH_3 conversion be x, the k can be expressed by Eq. (5).

$$\ln\left(\frac{1}{1-x}\right) = k \quad (5)$$

The apparent activation energy (Ea) and the frequency factor (A) for NH_3 decomposition over each catalyst were calculated from the Arrhenius plot in which the inverse of the reaction temperature ($1/T$) and k were plotted by Eq. (6).

$$\ln k = \ln A - \frac{Ea}{RT} \quad (6)$$

where R is the gas constant (8.314 J K mol^{-1}).

Arrhenius plots in NH_3 decomposition over the Ni and Co based catalysts are shown in Fig. S3. Since the linear relationship was obtained for all the catalysts, we consider that the NH_3 decomposition reaction was an apparent first reaction to NH_3 under this reaction condition (1% NH_3/Ar). The calculated apparent Ea and A of each catalyst from Arrhenius plot are summarized in Table 2. The Ea value for the Ni-Co/α-Al_2O_3 was 108 kJ mol^{-1} which was larger than those for the Co/α-Al_2O_3 and Ni/α-Al_2O_3 and the γ-Al_2O_3 supported catalysts also showed the similar tendency. According to the literature, it was reported that the Ea value of the Ni/CNTs catalyst for NH_3 decomposition was 90 kJ mol^{-1} (Yin et al., 2004b) and that of the Ni/SiO_2/Al_2O_3 catalyst was 92 kJ mol^{-1} (Choudhary et al., 2001). In addition, the Ea value of 110 kJ mol^{-1} was reported for zeolite supported Ni catalyst (Inokawa et al., 2015). For the supported catalyst for NH_3 decomposition, the Ea value is considered to vary due to the difference in active metal species and the support materials, and the modification effect of the third element, and the Ea values of *ca.* 53 to 150 kJ mol^{-1} was reported as literature data (Mukherjee et al., 2018). The A value for the Ni-Co/α-Al_2O_3 was 22.9 s^{-1} which was quite higher compared with those for the Ni/α-Al_2O_3 and Co/α-Al_2O_3. By contrast, although an increase in the A value was recognized, the difference in the A due to the binary metal was not large for the γ-Al_2O_3 supported catalysts. These results imply that the performance of the catalyst would greatly influence the frequency factor, that is, the number of active sites.

Table 2 Apparent activation energy and frequency factor for NH_3 decomposition over Ni and Co based catalysts

Catalyst	Activation energy, Ea (kJ mol^{-1})	Frequency factor, $A\times10^{-6}$ (s^{-1})
Co/γ-Al_2O_3	99	5.5
Ni/γ-Al_2O_3	111	36.0
Ni-Co/γ-Al_2O_3	115	70.6
Co/α-Al_2O_3	90	0.7
Ni/α-Al_2O_3	76	0.1
Ni-Co/α-Al_2O_3	108	22.9

2.6. Catalytic performance of other oxide supported Ni-Co catalysts

It is widely known that catalytic performance changes in the oxide supported metal catalysts due to the interaction between the active metal and the support. Therefore, to elucidate whether the improvement effect of the catalytic performance by alloying can be obtained for the other oxides used as a support, the Ni, Co, and Ni-Co catalysts with SiO_2 and TiO_2 supports (Co:Ni = 1:1) were prepared, and their NH_3 decomposition performance was evaluated. Fig. 10A shows the NH_3 decomposition performance of Ni/SiO_2, Co/SiO_2, and Ni-Co/SiO_2 catalysts, which is generally considered to have the weak metal-support interaction. The NH_3 conversion at 500 °C

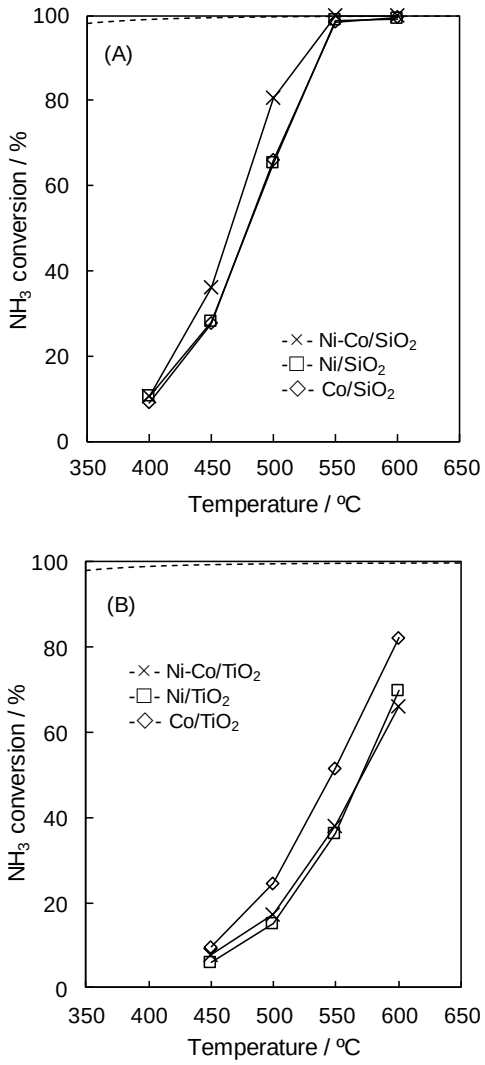

Fig. 10 NH_3 conversion for NH_3 decomposition over (A) SiO_2 and (B)TiO_2 supported Ni and Co based catalysts. Reaction conditions: 1.02% NH_3/Ar balance; W/F: 2.45 kg-cat s L-NH_3^{-1}; catalyst weight: 0.050 g. (dot-line) equilibrium NH_3 conversion.

was 65% for the Ni/SiO_2, 65% for the Co/SiO_2, and 80% for the Ni-Co/SiO_2, respectively. This indicates that the effect of improving the performance could be obtained for the Ni-Co binary metal catalyst even for the SiO_2 supported system with the similar trend as α-Al_2O_3 supported catalyst. And it is worth noting that the SiO_2-supported Ni-Co catalyst exhibited the higher performance than the α-Al_2O_3 supported Ni-Co catalyst.

By contrast, the Ni-Co catalyst using the TiO_2 (Fig. 10B) which has the strong metal support interaction (SMSI) showed the similar performance to single metal catalyst. For the γ-Al_2O_3 supported catalysts, there was no positive effect by alloying on the catalytic performance as shown in Fig. 3. And we noted that even if the loaded amounts of Ni and Co increased to the total of 40 wt%, these tendencies were the same (Fig. S4) for the γ-Al_2O_3 supported catalysts. But, the catalytic performance was improved by increasing the loading amount, namely, the 40 wt% Ni-Co/α-Al_2O_3 catalyst exhibited the NH_3 conversions of *ca.* 96% at 500 °C and of *ca.* 55% at 450 °C. From these results, we conclude that in the Ni and Co based catalyst system, the behavior of alloying of the metal component varies depending on the kind of the oxide support, which affects the catalytic performance of NH_3 decomposition.

Conclusion

In the present work, we have conducted the development of a base metal catalyst which shows high performance for the NH_3 decomposition reaction. For the Ni and Co based catalysts using α-Al_2O_3 as a support, the performance of the single metal catalysts was lower than that of the γ-Al_2O_3 supported catalysts. However, its performance was greatly improved by using a binary metal catalyst. Based on the XRD analysis, it was found that Ni and Co supported on α-Al_2O_3 were alloyed. TEM observation confirmed that the metal particle size in the α-Al_2O_3 supported Ni-Co catalyst is smaller than that of the single metal catalysts (Ni/α-Al_2O_3 or Co/α-Al_2O_3). The optimum mixing ratio of Ni and Co components was 1:1, and the optimum reduction temperature before the test was 600 °C. Furthermore, *in-situ* XRD and H_2-TPR measurements revealed that the Ni-Co alloy forms during the reduction process. Studies on the differences of support oxides proved that the improvement effect by alloying can be similarly obtained with the SiO_2 supported catalyst, indicating that the catalyst using the support with

less interaction between the active metal and the support is more likely to obtain the performance improvement effect by alloying.

Acknowledgments

TEM analysis was supported by the Cooperative Research Program of Catalysis Research Center, Hokkaido University (Grant 14B1009).

Literature Cited

Becherif, M., Claude, F., Hervier, T. and Boulon, L.; "Multi-stack Fuel Cells Powering a Vehicle," *Energy Procedia*, **74,** 308-319 (2015)

Choi, J.-G.; "Ammonia Decomposition over Vanadium Carbide Catalysts," *J. Catal.*, **182,** 104-116 (1999)

Choudhary, T. V., Sivadinarayana, C. and Goodman, D. W.; "Catalytic ammonia decomposition: COx-free hydrogen production for fuel cell applications," *Catal. Lett.*, **72,** 197-201 (2001)

Deng, Q.-F., Zhang, H., Hou, X.-X., Ren, T.-Z. and Yuan, Z.-Y.; "High-surface-area $Ce_{0.8}Zr_{0.2}O_2$ solid solutions supported Ni catalysts for ammonia decomposition to hydrogen," *Int. J. Hydrogen Energy*, **37,** 15901-15907 (2012)

Duan, X., Ji, J., Qian, G., Fan, C., Zhu, Y., Zhou, X., Chen, D. and Yuan, W.; "Ammonia decomposition on Fe(110), Co(111) and Ni(111) surfaces: A density functional theory study," *J. Mol. Catal. A: Chem.*, **357,** 81-86 (2012)

Duan, X., Qian, G., Liu, Y., Ji, J., Zhou, X., Chen, D. and Yuan, W.; "Structure sensitivity of ammonia decomposition over Ni catalysts: A computational and experimental study," *Fuel Process. Technol.*, **108,** 112-117 (2013)

Ertl, G. and Huber, M.; "Mechanism and Kinetics of Ammonia Decomposition on Iron," *J. Catal.*, **61,** 537-539 (1980)

Gonzalez-delaCruz, V. M., Pereñiguez, R., Ternero, F., Holgado, J. P. and Caballero, A.; "In Situ XAS Study of Synergic Effects on Ni–Co/ZrO_2 Methane Reforming Catalysts," *The Journal of Physical Chemistry C*, **116,** 2919-2926 (2012)

Hashimoto, K. and Toukai, N.; "Decomposition of ammonia over a catalyst consisting of ruthenium metal and cerium oxides supported on Y-form zeolite," *J. Mol. Catal. A: Chem.*, **161,** 171-178 (2000)

Hayashi, F., Toda, Y., Kanie, Y., Kitano, M., Inoue, Y., Yokoyama, T., Hara, M. and Hosono, H.; "Ammonia decomposition by ruthenium nanoparticles loaded on inorganic electride C12A7:e^-," *Chemical Science*, **4,** 3124-3130 (2013)

Huang, D.-C., Jiang, C.-H., Liu, F.-J., Cheng, Y.-C., Chen, Y.-C. and Hsueh, K.-L.; "Preparation of Ru–Cs catalyst and its application on hydrogen production by ammonia decomposition," *Int. J. Hydrogen Energy*, **38,** 3233-3240 (2013)

Inokawa, H., Ichikawa, T., Miyaoka, H.; "Catalysis of nickel nanoparticles with high thermal stability forammonia decomposition," *Appl. Catal. A: General*, **491,** 184-188 (2015)

Li, L., Zhu, Z. H., Yan, Z. F., Lu, G. Q. and Rintoul, L.; "Catalytic ammonia decomposition over Ru/carbon catalysts: The importance of the structure of carbon support," *Applied Catalysis A: General*, **320,** 166-172 (2007)

Liang, C., Li, W., Wei, Z., Xin, Q. and Li, C.; "Catalytic Decomposition of Ammonia over Nitrided MoN*x*/γ-Al_2O_3

and NiMoN*y*/γ-Al_2O_3 Catalysts," *Ind. Eng. Chem. Res.*, **39,** 3694-3697 (2000)

Liu, Y., Wang, H., Li, J., Lu, Y., Wu, H., Xue, Q. and Chen, L.; "Monolithic microfibrous nickel catalyst co-modified with ceria and alumina for miniature hydrogen production via ammonia decomposition," *Applied Catalysis A: General*, **328,** 77-82 (2007)

Luisetto, I., Tuti, S. and Di Bartolomeo, E.; "Co and Ni supported on CeO_2 as selective bimetallic catalyst for dry reforming of methane," *Int. J. Hydrogen Energy*, **37,** 15992-15999 (2012)

Mukherjee, S., Devaaguptapu, S.V., Sviripa, A.,

Lund, C.R.F., Wu, G.; “Low-temperature ammonia decomposition catalysts for hydrogen generation,” *Appl. Catal. B: Environmental.*, **226,** 162-181 (2018)

Muñoz, M., Moreno, S. and Molina, R.; "The effect of the absence of Ni, Co, and Ni–Co catalyst pretreatment on catalytic activity for hydrogen production via oxidative steam reforming of ethanol," *Int. J. Hydrogen Energy*, **39,** 10074-10089 (2014)

Nagaoka, K., Eboshi, T., Abe, N., Miyahara, S.-i., Honda, K. and Sato, K.; "Influence of basic dopants on the activity of Ru/Pr_6O_{11} for hydrogen production by ammonia decomposition," *Int. J. Hydrogen Energy*, **39,** 20731-20735 (2014)

Nagaoka, K., Honda, K., Ibuki, M., Sato, K. and Takita, Y.; "Highly Active $Cs_2O/Ru/Pr_6O_{11}$as a Catalyst for Ammonia Decomposition," *Chem. Lett.*, **39,** 918-919 (2010)

Okura, K., Okanishi, T., Muroyama, H., Matsui, T. and Eguchi, K.; "Promotion effect of rare-earth elements on the catalytic decomposition of ammonia over Ni/Al_2O_3 catalyst," *Applied Catalysis A: General*, **505,** 77-85 (2015)

Raróg-Pilecka, W., Szmigiel, D., Kowalczyk, Z., Jodzis, S. and Zielinski, J.; "Ammonia decomposition over the carbon-based ruthenium catalyst promoted with barium or cesium," *J. Catal.*, **218,** 465-469 (2003)

Sato, K., Abe, N., Kawagoe, T., Miyahara, S.-i., Honda, K. and Nagaoka, K.; "Supported Ni catalysts prepared from hydrotalcite-like compounds for the production of hydrogen by ammonia decomposition," *Int. J. Hydrogen Energy*, **42,** 6610-6617 (2017)

Saw, E. T., Oemar, U., Tan, X. R., Du, Y., Borgna, A., Hidajat, K. and Kawi, S.; "Bimetallic Ni–Cu catalyst supported on CeO_2 for high-temperature water–gas shift reaction: Methane suppression via enhanced CO adsorption," *J. Catal.*, **314,** 32-46 (2014)

Sengupta, S., Ray, K. and Deo, G.; "Effects of modifying Ni/Al_2O_3 catalyst with cobalt on the reforming of CH_4 with CO_2 and cracking of CH_4 reactions," *Int. J. Hydrogen Energy*, **39,** 11462-11472 (2014)

Shimoda, N., Koide, N., Kasahara, M., Mukoyama, T. and Satokawa, S.; "Development of oxide-supported nickel-based catalysts for catalytic decomposition of dimethyl sulfide," *Fuel*, **232,** 485-494 (2018)

Yin, S.-F., Xu, B.-Q., Ng, C.-F. and Au, C.-T.; "Nano Ru/CNTs: a highly active and stable catalyst for the generation of CO*x*-free hydrogen in ammonia decomposition," *Applied Catalysis B: Environmental*, **48,** 237-241 (2004a)

Yin, S.-F., Xu, B.-Q., Wang, S.-J. and Au, C.-T.; "Nanosized Ru on high-surface-area superbasic ZrO_2-KOH for efficient generation of hydrogen via ammonia decomposition," *Applied Catalysis A: General*, **301,** 202-210 (2006)

Yin, S.-F., Zhang, Q.-H., Xu, B.-Q., Zhu, W.-X., Ng, C.-F. and Au, C.-T.; "Investigation on the catalysis of COx-free hydrogen generation from ammonia," *J. Catal.*, **224,** 384-396 (2004b)

Zhang, J., Xu, H., Ge, Q. and Li, W.; "Highly efficient Ru/MgO catalysts for NH_3 decomposition: Synthesis, characterization and promoter effect," *Catal. Commun.*, **7,** 148-152 (2006)